Vehicle Localization Using Joint DOA/TOA Estimation Based on TLS-ESPRIT Algorithm

Shanjie Zhang[1(✉)], Yi Shi[1], Rui Zhang[2], Feng Yan[2], Yi Wu[3], Weiwei Xia[2], and Lianfeng Shen[2]

[1] Collaborative Innovation Center of Advanced Microstructures, Nanjing University, Nanjing 210093, People's Republic of China
mf1623045@smail.nju.edu.cn, yshi@nju.edu.cn
[2] National Mobile Communications Research Laboratory, Southeast University, Nanjing 210096, People's Republic of China
{zhangrui09, feng.yan, wwxia, lfshen}@seu.edu.cn
[3] Key Laboratory of OptoElectronic Science and Technology for Medicine of Ministry of Education, Fujian Provincial Key Laboratory of Photonics Technology, Fujian Normal University, Fuzhou 350007, People's Republic of China
wuyi@fjnu.edu.cn

Abstract. In this paper, a high-resolution vehicle positioning estimation algorithm based on existing Vehicle to Infrastructure (V2I) communications is proposed to achieve joint estimation of vehicle target's direction of arrival (DOA) and time of arrival (TOA). We adopt the Estimating Signal Parameters via Rotational Invariance Techniques (ESPRIT) algorithm based on total least squares (TLS) to estimate the DOA and TOA, and the vehicle location can be obtained from the estimated parameters. The TLS-ESPRIT algorithm not only has a relatively small amount of computation to meet the real-time requirements of vehicle localization, but also has the advantage of strong anti-noise. We also introduce unscented Kalman filter (UKF) to further improve the localization accuracy of the TLS-ESPRIT algorithm and to reduce the influence of noise interference. The simulation results show that compared with the traditional 2D-ESPRIT parameter estimation methods without UKF and the Global Positioning System (GPS), this method has better performance of positioning parameter estimation.

Keywords: Vehicle location · TLS-ESPRIT · Direction of arrival (DOA) · Arrival time (TOA) · Kalman filter

1 Introduction

With the rapid development of intelligent transportation system (ITS), many emerging application techniques appear in the Internet of Vehicles, such as traffic flow control, road safety, automatic driving, and Vehicle queuing Network [1]. The realization of these applications can not be separated from the accurate and reliable perception of the vehicle position information. Currently, different positioning methods can be used for the precise positioning of the traveling vehicle. One of the most widely used

© ICST Institute for Computer Sciences, Social Informatics and Telecommunications Engineering 2019
Published by Springer Nature Switzerland AG 2019. All Rights Reserved
M. Jia et al. (Eds.): WiSATS 2019, LNICST 281, pp. 297–309, 2019.
https://doi.org/10.1007/978-3-030-19156-6_28

positioning methods is the Global Navigation Satellite System (GNSS) represented by Global Positioning System (GPS). Its positioning error is generally about 10 m, and the best positioning accuracy that the GPS positioning method can achieve after optimization is between 3 m to 7 m, such as differential GPS [2]. However, the positioning accuracy of GPS is affected by the use environment. For example, in an occluded urban environment or a high-speed driving scene, due to the presence of unstable factors such as signal multipath and target driving speed, the positioning error will be greatly increased to 15 m [3, 4]. Therefore, in ITS, the accuracy of satellite positioning does not satisfy the need for more precise positioning within one meter in applications such as collaborative driving or collision avoidance [5]. However, it is also possible to use roadside unit (RSU) positioning based on Dedicated Short-Range Communication (DSRC) to meet the requirements of ITS positioning accuracy. Therefore, vehicle positioning parameter estimation algorithm for obtaining a wireless positioning signal by communicating with the RSU has the significance of research.

The RSU serves as pre-deployed road facilities and provides positioning parameters such as Received Signal Strength (RSS), Time of Arrival (TOA) and Direction of Arrival (DOA) through communication between the vehicle and roadside infrastructure (V2I). For wireless access in vehicular environment (WAVE), dedicated short range communications (DSRC) technology is one of the earliest developed and most mature communication technology. It supports wireless access based on the IEEE 802.11p protocol to provide high-speed, low-latency inter-vehicle and vehicle-to-infrastructure communication services [6], and spreads orthogonal frequency division multiplexing (OFDM) signal in its radio channel [7]. Therefore, the estimation of the positioning parameters contained in signals such as DOA and TOA is an important research content in vehicle positioning. Joint DOA/TOA parameter estimation has many advantages, not only can improve the positioning accuracy through multiple roadside unit coverage, but also can greatly reduce the number of deployment of roadside nodes compared to a single positioning parameter estimation. Theoretically, only one roadside node can be used to locate the target vehicle [8]. In a super-resolution channel parameter estimation method based on a Uniform Linear Array (ULA), the ESPRIT algorithm has many performance advantages over the Multiple Signal Classification (MUSIC) algorithm. For example, the DOA estimation accuracy and computational complexity are significantly better than the MUSIC algorithm [9], and no two-dimensional spatial peak search is needed. In addition, the two-dimensional matrix pencil (2D-MP) proposed in [10] is a direct data-domain method that does not require calculation of signal covariance matrix, but the disadvantage of this method is that three or more RSUs are needed to provide Sufficient range reference signal.

The novelty of this paper is to propose a low-complexity ESPRIT algorithm based on Total least squares (TLS). Joint parameter estimation of DOA and TOA is achieved by analyzing multipath channel frequency response (CFR) of OFDM signals. In addition, unscented Kalman filter (UKF) is also used to reduce the channel noise interference to improve the joint parameter estimation accuracy. At low signal-to-noise ratio (SNR), the proposed TLS-ESPRIT algorithm overcomes the disadvantages of poor positioning accuracy of multi-signal classification and its real-time performance is much better than the MUSIC algorithm. The precise position information of vehicle is finally obtained by recombining the velocity components through joint observations of

DOA and TOA. This article is organized in the following order: Sect. 2 provides a vehicle positioning system model. The proposed calculation principles of the TLS-ESPRIT localization algorithm and the UKF filtering algorithm are described in Sect. 3. Section 4 discusses the performance of the algorithm and simulation results. Finally, the Sect. 5 is the summary of this article and the discussion of the follow-up tasks.

2 Positioning System Model

It is assumed that the roadside node units have been pre-deployed in the vehicle positioning system beside the bidirectional lanes, and that the communication distances of these roadside unit sets can cover the entire road, and the position information of these roadside units is known to the vehicle. In this system, both the roadside unit and the vehicle are equipped with DSRC terminal equipment, so the V2I communication between the roadside unit and the vehicle is accomplished through the 802.11P protocol. A multi-antenna array is also installed at the driving vehicle to detect the frequency response of the multi-path channel of the received OFDM signal. In addition, the vehicle can also obtain the current speed vector data through the navigation or speed sensor device carried by itself. The location scenario of driving vehicles in an urban environment is shown in Fig. 1.

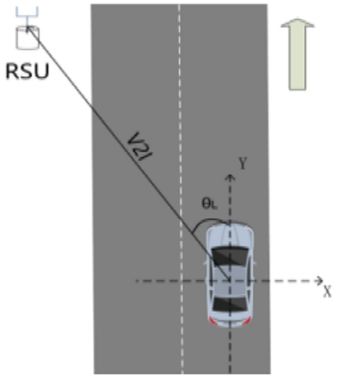

Fig. 1. RSU-based vehicle location scenario

In addition, the on-board unit is also equipped with an M antenna receiving array. We assume that the antenna array spacing is a fixed value and is generally half of the signal wavelength. The transmitted signal $S_T(t)$ is received by the antenna array via L propagation paths, only one of which is along the line of sight (LOS) and others are considered as non-line-of-sight propagation. According to [11], the time domain signal received by the mth antenna element in a uniform linear array (ULA) can be expressed as:

$$S_{\mathrm{m},k}(t) = \sum_{l=1}^{L} e^{\frac{-j2\pi d(m-1)\sin\theta_l}{\lambda_k}} \beta_l S_T(t-\tau_l) + N_{m,k}(t) \tag{1}$$

In (1), the interval of ULA is $d_1 = d_2 = d_3 = \cdots = d_{M-1} = d$. λ_k is the kth subcarrier wavelength of the OFDM signal, β_l is the complex attenuation coefficient of different paths, and $S_T(t-\tau_l)$ is the signal transmitted by the roadside unit. θ_l, τ_l corresponds to DOA and TOA for different propagation paths, respectively. $N_{m,k}$ is the zero mean additive white Gaussian noise (AWGN) of different subcarriers on different antennas. In [12], the complex time domain received signals of different antennas can also be expressed as:

$$S_{\mathrm{m},k} = \sum_{l=1}^{L} \beta_l e^{-j2\pi\left\{d(m-1)\frac{\sin\theta_l}{\lambda_k} + [f_D + (k-1)f_S]\tau_l\right\}} + N_{m,k} \tag{2}$$

Where f_D is the Doppler frequency shift, f_S is the subcarrier frequency interval, and k is the number of subcarriers of the OFDM signal, in the range of [1 ,⋯, K]. The antenna index value m is in the range [1 ,⋯, M], the propagation path of the OFDM signal is shown in Fig. 2.

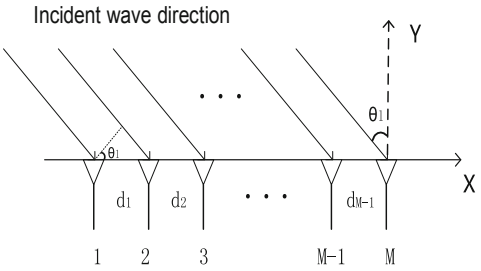

Fig. 2. Antenna array receive signal diagram

In (2), $d(m-1)\frac{\sin\theta_l}{\lambda_k}$ denotes the phase difference between the mth antenna element in the ULA and the reference array element due to the propagation path difference. According to [13], we rewrite $S_{\mathrm{m,\,k}}$ into a vector form:

$$S = H\beta_l + n \tag{3}$$

In (3), H denotes the transmission channel matrix, β_l is the path-dependent complex attenuation coefficient vector, and $[]^{\mathrm{T}}$ denotes the transposition of the vector.

$$S(n) = [s_1(n), s_2(n), s_3(n), \cdots, s_M(n)]^{\mathrm{T}}$$

$$n(n) = [n_1(n), n_2(n), n_3(n), \cdots, n_M(n)]^{\mathrm{T}}$$

$$H = \begin{bmatrix} h_{1,1}(\theta_1,\tau_1) & h_{1,2}(\theta_2,\tau_2) & \cdots & h_{1,L}(\theta_L,\tau_L) \\ h_{2,1}(\theta_1,\tau_1) & h_{2,2}(\theta_2,\tau_2) & \cdots & h_{2,L}(\theta_L,\tau_L) \\ \vdots & \vdots & \ddots & \vdots \\ h_{M,1}(\theta_1,\tau_1) & h_{M,2}(\theta_2,\tau_2) & \cdots & h_{M,L}(\theta_L,\tau_L) \end{bmatrix}$$

$$h_{M,L}(\theta_L,\tau_L) = e^{-j2\pi\left\{d(M-1)\frac{\sin\theta_L}{\lambda_k} + [f_D + (k-1)f_S]\tau_L\right\}}$$

$$\beta_l = [\beta_1, \beta_2, \beta_3, \cdots, \beta_L]^{\mathrm{T}}$$

Then the total least squares algorithm (TLS-ESPRIT) is used to jointly estimate the DOA and TOA of the received signal, and then use UKF to further optimize the estimation result.

3 Parameter Estimation Algorithm

3.1 Total Least Squares Based ESPRIT Algorithm (TLS-ESPRIT)

In the parameter estimation of the received signal, it is assumed that the number of antennas M of the ULA at the receiving end is greater than the multipath number L of signal propagation, and the former [1: $M-1$] array antennas and the last [2: M] arrays in Fig. 2 are taken respectively. The elements form two sub-antenna arrays. By default, the first sub-array receives the signal vector S_1(n), and the second sub-array receives the signal vector S_2(n). Available from (3):

$$S_1 = [s_1(n), s_2(n), s_3(n), \cdots, s_{M-1}(n)]^{\mathrm{T}} = H_1.\beta_l + n_1 \tag{4}$$

$$S_2 = [s_2(n), s_3(n), s_4(n), \cdots, s_M(n)]^{\mathrm{T}} = H_2.\beta_l + n_2 \tag{5}$$

In (4) and (5), the matrice H_1, H_2 are

$$H_1 = \begin{bmatrix} h_{1,1}(\theta_1,\tau_1) & h_{1,2}(\theta_2,\tau_2) & \cdots & h_{1,L}(\theta_L,\tau_L) \\ h_{2,1}(\theta_1,\tau_1) & h_{2,2}(\theta_2,\tau_2) & \cdots & h_{2,L}(\theta_L,\tau_L) \\ \vdots & \vdots & \ddots & \vdots \\ h_{M-1,1}(\theta_1,\tau_1) & h_{M-1,2}(\theta_2,\tau_2) & \cdots & h_{M-1,L}(\theta_L,\tau_L) \end{bmatrix}$$

$$H_2 = \begin{bmatrix} h_{2,1}(\theta_1,\tau_1) & h_{2,2}(\theta_2,\tau_2) & \cdots & h_{2,L}(\theta_L,\tau_L) \\ h_{2,1}(\theta_1,\tau_1) & h_{2,2}(\theta_2,\tau_2) & \cdots & h_{2,L}(\theta_L,\tau_L) \\ \vdots & \vdots & \ddots & \vdots \\ h_{M,1}(\theta_1,\tau_1) & h_{M,2}(\theta_2,\tau_2) & \cdots & h_{M,L}(\theta_L,\tau_L) \end{bmatrix}$$

Thus, (5) can be written as:

$$S_2 = H_1 \Phi \beta_l + n_2 \tag{6}$$

$$\Phi = diag\left\{e^{-2\pi j\alpha_1}, e^{-2\pi j\alpha_2}, \cdots, e^{-2\pi j\alpha_L}\right\} \tag{7}$$

$$\alpha_l = d \times \sin\theta_l/\lambda_k + f_s \times \tau_l, l = 1, \cdots, L \tag{8}$$

The DOA and TOA of the incident multipath signal are included in the diagonal matrix Φ. If the corresponding rotation-invariant relationship between the subarrays can be obtained, the vehicle positioning information can be extracted. Combine S_1 and S_2 into a new matrix S_3.

$$S_3 = \begin{bmatrix} S_1 \\ S_2 \end{bmatrix} = \begin{bmatrix} H_1 \\ H_1 \bullet \Phi \end{bmatrix} \beta_l + \begin{bmatrix} n_1 \\ n_2 \end{bmatrix} = \widehat{H}\, \beta_l + \widehat{n} \tag{9}$$

Solving the Autocorrelation Matrix of S_3 in (9).

$$R_{S_3} = E[S_3\, S_3^{\mathrm{T}}] = \widehat{H}\, R_{\beta_l}\, \widehat{H}^{\mathrm{H}} + \delta^2 N \tag{10}$$

In the above formula, $(.)^{\mathrm{H}}$ represents the Hermitian transpose, $R_{\beta_l} = E[\beta_l\, \beta_l^{\mathrm{H}}]$ and δ^2 is the variance of Gaussian white noise. $N = \begin{bmatrix} E_{M-1} & J \\ J^H & E_{M-1} \end{bmatrix}$, E_{M-1} is an $M-1$ order identity matrix, and J is a $M-1$ order square matrix with all subdiagonals of 1.

Solving the generalized eigenvalues of R_{S3} results in $\lambda_1 \geq \lambda_2 \geq \cdots \geq \lambda_L \geq \lambda_{L+1} = \cdots = \lambda_{2M-2} = \delta^2$. Let the eigenvectors of the first L corresponding large generalized eigenvalues make up the signal subspace $I = [I_1, I_2, \cdots, I_L]$, because the columns of the matrix I and the columns of the direction matrix can be expanded into the same subspace:

$$\text{span}\{I\} = \text{span}\left\{\hat{H}\right\} \tag{11}$$

so there is a unique $L \times L$ order non-singular matrix A such that

$$I = \widehat{H} \times A \tag{12}$$

decompose the signal subspace I into two $M-1 \times L$ matrices I_1, I_2, where $I_1 = H_1\, A, I_2 = H_1\, \Phi A$, and construct the $M-1 \times 2L$ matrix $I_{12} = [I_1, I_2]$, from which $(I_{12})^{\mathrm{H}} \times I_{12}$ is obtained:

$$\begin{bmatrix} I_1^{\mathrm{H}} \\ I_2^{\mathrm{H}} \end{bmatrix} [I_1 \quad I_2] = \begin{bmatrix} A^{\mathrm{H}} \\ A^{\mathrm{H}} \Phi^{\mathrm{H}} \end{bmatrix} H_1^{\mathrm{H}} H_1 [A \quad \Phi A] \tag{13}$$

Solve the eigenvalues of the (13) and their corresponding eigenvectors, and sort the eigenvalues from largest to smallest $\Lambda_1 \geq \Lambda_2 \geq \ldots \geq \Lambda_L \geq \Lambda_{L+1} = \ldots = \Lambda_{2L} = 0$,

corresponding the feature vectors are u_1, u_2,…, u_L,…, u_{2L}. So (13) can also be expressed as

$$(I_{12})^H \times I_{12} = U \Lambda U^H \tag{14}$$

In (14), Λ is a diagonal matrix consisting of eigenvectors. U is a $2L \times 2L$ square matrix and is divided into blocks as follows.

$$U = \begin{bmatrix} U_{11} & U_{12} \\ U_{21} & U_{22} \end{bmatrix} \tag{15}$$

available by (15)

$$A^{-1} \Phi A = -U_{12} U_{22}^{-1} \tag{16}$$

The eigenvalue decomposition on the right side of the equal sign of (16) results in L eigenvalues g_1, g_2, ⋯, g_L. The DOA and TOA of the target vehicle are given by the following formula:

$$\widehat{\tau}_l = \frac{-\arg(g_l)}{2\pi f_S} \tag{17}$$

$$\widehat{\theta}_l = \arcsin\left[\frac{-\arg(g_l)\lambda}{2\pi d}\right] \tag{18}$$

In (18), λ is the carrier wavelength of the received signal, so the position information of the vehicle can be accurately measured by (17), (18). The proposed 2D-ELSITE algorithm achieves automatic pairing by joint diagonalization of DOA and TOA parameters, which can effectively overcome the problem of degraded estimation performance of the 1D-ESPRIT algorithm caused by changes in the carrier frequency offset caused by the mobility of the target vehicle [16].

3.2 Unscented Kalman Filter (UKF)

The essence of Kalman filtering is to reconstruct the state vector of the positioning system from the measured values. According to the measurement value of the vehicle positioning system, the noise interference is filtered out from the noise-polluted system, and the estimated performance degradation under low SNR environment can be overcome. Unscented Kalman filter (UKF) is a method that approximates nonlinear distribution using sigma points and is based on UT (Unscented Transform) transformation. Compared with the extended Kalman filter (EKF), UKF does not approximate the nonlinear function and there is no defect caused by omitting Taylor's expansion of higher-order terms, which increases the estimation accuracy and robustness of strongly nonlinear systems [15]. The UKF proposed in this paper can not only reduce the channel noise and the influence of estimation error, but also predict the DOA and TOA

of the next moment of the vehicle through the velocity component. The UKF filtered system equation is given by:

$$\begin{cases} X(k) = FX(k-1) + Gw(k-1) \\ Z(k) = h[X(k)] + u(k) \end{cases} \tag{19}$$

In (19), $X(k)$ is N rows state column vector, $Z(k)$ is M rows observation column vector, $w(k)$, $u(k)$ are zero mean Gaussian state noise and Gaussian observation noise, F is an $N \times N$ state transition matrix, G is the noise input matrix of the system, and h is a nonlinear transformation function, i.e., $E^{N\times 1} \Rightarrow E^{M\times 1}$. If the state vector of the sigma sample point at time k is $X_S(k|k)$, the one-step state estimation and observation estimation formula of the sample point at $k-1$ time is:

$$\begin{cases} X_S(k|k-1) = F\bullet\ X_S(k-1) \\ Z_S(k|k-1) = h[X_S(k-1)] \end{cases} \tag{20}$$

A one-step prediction of the system state estimation and state covariance estimation of UKF is:

$$\begin{cases} X(k|k-1) = \sum_{S=0}^{2n} W_S\, X_S(k|k-1) \\ A(k|k-1) = \sum_{S=0}^{2n} W_S\, X'\bullet\ X'^T \end{cases} \tag{21}$$

In (21), $X' = X(k|k-1) - X_S(k|k-1)$, the one-step prediction of the observational estimation and observation covariance estimation is:

$$\begin{cases} Z(k|k-1) = \sum_{S=0}^{2n} W_S\, Z_S(k|k-1) \\ B(k|k-1) = \sum_{S=0}^{2n} W_S\, Z' \times Z'^T \end{cases} \tag{22}$$

In (22), $Z' = Z(k|k-1) - Z_S(k|k-1)$, the full state vector of UKF and the state covariance can be expressed as:

$$\begin{cases} K(k) = \frac{A(k|k-1)}{B(k|k-1)} \\ X(k) = X(k|k-1) + K(k)[Z(k) - Z(k|k-1)] \\ A(k) = A(k|k-1) - K(k)B(k|k-1)\, K^T(k) \end{cases} \tag{23}$$

In (23), $K(k)$ denotes the Kalman gain. In (21) and (22), W_S denotes the weights of different *sigma* points. The DOA and TOA components in the initial state vector X(0) can be obtained by (17) and (18), we also let the UKF state vector be:

$$X(k) = [\theta(k), \tau(k), V_X(k), V_Y(k)]^T \tag{24}$$

$\theta(k), \tau(k)$ respectively represent the DOA and TOA of the LOS path at time k, and V_X and V_Y are the traveling speeds in the X and Y directions in Fig. 1, respectively.

4 Simulation Results

This paper proposes that TLS-based positioning estimation algorithm needs a 2M-2 × 2M-2 order, once 2L × 2L order and L × L order eigenvalue decomposition. In practical applications, the computational complexity is also related to the number of samples N in digital signal processing. It can be approximated as O(N3) [14]. In this simulation, the proposed algorithm with and without UKF filters were simulated in the vehicle location scenario, and GPS was added for comparison. The vehicle positioning accuracy based on DOA and TOA estimation was studied, and the effectiveness of parameter estimation using UKF was illustrated. The vehicle's positioning scenario is that the vehicle travels along a road with a length of about 1 km and a width of 10 m at a constant speed and Simulation parameters for vehicle position estimation are shown in Table 1.

Table 1. Simulation parameters

Parameter	Numeric value
Multipath number	4
Number of receiving antennas	12
Antenna spacing	Half the wavelength
Center frequency	5.9 GHz
Bandwidth	10 MHz
Number of subcarriers	24
Speed of vehicle	30 m/s
Road length and width	1000 m/10 m
Input SNR	50 db

Vehicle tracking is achieved at the vehicle using a vehicle-mounted ULA array to receive broadcast packets and extract the DOA/TOA of LOS through the 2D-ESPRIT algorithm.

In the simulation, we continuously track the vehicle for more than 30 s. We record the position information generated by the DOA/TOA parameter estimation method with and without the UKF filter and the GPS positioning method in the Y direction and the X direction, respectively. The evaluation criterion of the positioning simulation is the positioning accuracy error, that is, the absolute value of the difference between the estimated position and the actual position of the Y-X axis coordinate. The simulation results of the Y-X axis are shown in Figs. 3 and 4 below:

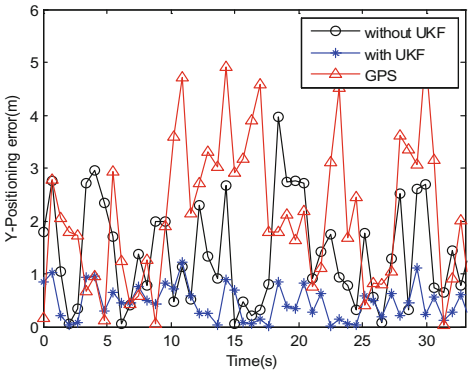

Fig. 3. Positioning accuracy of the DOA/TOA estimation method on the Y-axis

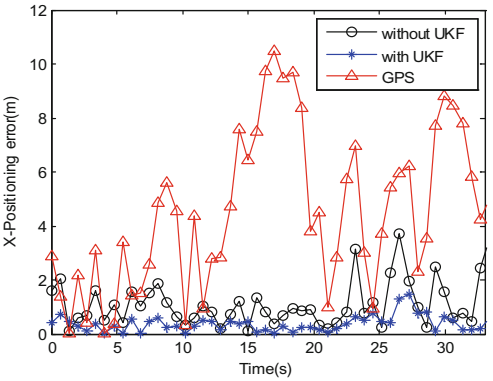

Fig. 4. Positioning accuracy of the DOA/TOA estimation method on the X-axis

In Figs. 3 and 4 above, the positioning error between the conventional 2D-ESPRIT estimation algorithm without UKF, the GPS positioning and the proposed positioning estimation algorithm in the Y and X directions are respectively shown to change over time. As shown in Fig. 3, in the Y direction (traveling direction), the positioning error of the conventional 2D-ESPRIT algorithm without UKF varies significantly within a range of 3 m with time. In addition, the GPS positioning is affected by measurement noise in various aspects and the positioning error is even up to about 5 m. While the accuracy of the proposed positioning algorithm with UKF doesn't fluctuate with time, and the positioning accuracy can remain stable during the tracking period, about 1 m. Figure 4 shows that in the X direction, the positioning accuracy of the algorithm presented in this paper can remain stable over time, and its error reaches a decimeter level around 0.5 m. The accuracy of the conventional estimation algorithm without UKF in the early stage is slightly inferior to the algorithm proposed in this paper. However, since the vehicle is far away from the RSU, accuracy loss is caused in the later period. The accuracy loss of GPS is more obvious with time and it can no longer

meet the application requirements. Therefore, the positioning estimation algorithm with UKF proposed in this paper has much better performance than the traditional two-dimensional subspace estimation algorithm and the GPS positioning in the resolution and stability of location accuracy.

In addition to the above criteria, this paper also uses two-dimensional Euclidean distance to represent the estimated error of position coordinates, i.e., from which the probability distribution of the error can be obtained. The cumulative distribution function (CDF) of the estimated error generated by the UKF filtering positioning algorithm is as shown in Fig. 5.

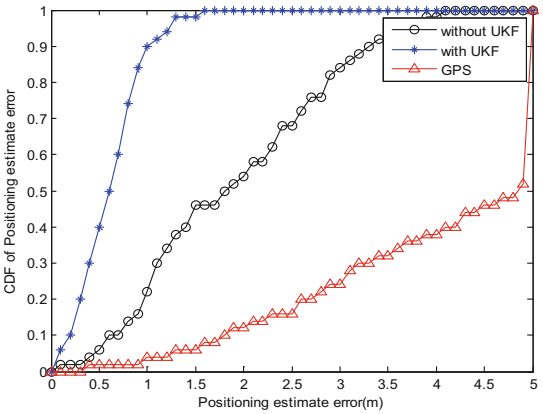

Fig. 5. Cumulative distribution function (CDF) generated by different localization algorithms

The above figure shows that the proposed ESPRIT estimation algorithm with UKF has absolute advantages over traditional algorithms and GPS in terms of reliability. For example, the proposed positioning algorithm can make the error value of the 98% vehicle positioning sample less than 1.5 m. However, if the vehicle positioning using the traditional 2D-ESPRIT estimation algorithm and making the estimation error within 1.5 m, the percentage can only reach 46%, and the percentage of GPS positioning to achieve the same positioning error standard is even lower, only 6%.

5 Conclusion

We propose a vehicle location algorithm based on DOA/TOA joint estimation in this paper. The ESPRIT algorithm utilizes the rotation invariance of the ULA received signal and performs super-resolution estimation of the spatial spectrum through the principle of total least squares (TLS). Different from the traditional two-dimensional spatial spectrum estimation algorithm, the proposed algorithm also introduces the Unscented Kalman Filter (UKF) to overcome the noise interference in the V2I communication environment, which greatly improves the accuracy and reliability of DOA and TOA estimation. Therefore, it is possible to obtain fairly accurate vehicle

positioning information to meet the demand for high-precision positioning by the Intelligent connected vehicle. In addition, our follow-up work will also in-depth study of the number of ULA elements, RSU coverage dimensions and real-time constraints and other conditions on the vehicle positioning accuracy, in order to achieve the vehicle positioning accuracy optimization.

Acknowledgment. This work is supported in part by the National Natural Science Foundation of China (No. 61571128, 61471164, 61601122 and 61741102).

References

1. Kumar, V., Mishra, S., Chand, N.: Applications of VANETs: present & future. In: International Conference on Wireless Communications, NETWORKING and Mobile Computing-Wicom 2012, vol. 5, no. 01, pp. 1780–1788, September 2013
2. Chia-Ho, O.: A roadside unit-based localization scheme for vehicular ad hoc networks. Int. J. Commun. Syst. **27**(1), 135–150 (2014)
3. Modsching, M., Kramer, R., ten Hagen, K.: Field trial on GPS accuracy in a medium size city: the influence of built-up. In: 3rd Workshop on Positioning, Navigation and Communication, pp. 209–218, April 2006
4. Younis, H.K., Ahmad, R.B., AlRawi, A.A.A.: Impact of multipath interference and change of velocity on the reliability and precision of GPS. In: 2014 2nd International conference on Electronic Design (ICED), Penang, Malaysia, pp. 427–430, August 2014
5. Boukerche, A., Oliveira, H., Nakamura, E.F., Loureiro, A.: Vehicular ad hoc networks: a new challenge for localization based systems. Comput. Commun. **31**(12), 2838–2849 (2008)
6. Zeadally, S., Hunt, R., Chen, Y.S., Irwin, A., Hassan, A.: Vehicular ad hoc networks (VANETs): status, results, and challenges. Telecommun. Syst. **50**(4), 217–241 (2012)
7. Elazab, M., Noureldin, A., Hassanein, H.S.: Integrated cooperative localization for connected vehicles in urban canyons. In: Proceedings of IEEE GlobeCom, San Diego, CA, USA, pp. 1–6, December 2015
8. Sarkar, T., Ji, Z., Kim, K., Medouri, A., Salazar-Palma, M.: A survey of various propagation models for mobile communication. IEEE Ant. Prop. Mag. **45**(3), 51–82 (2003)
9. Vikas, B., Vakula, D.: Performance comparision of MUSIC and ESPRIT algorithms in presence of coherent signals for DoA estimation. In: International Conference on Electronics, Communication and Aerospace Technology, pp. 403–405, April 2017
10. Gaber, A., Omar, A.: A study of wireless indoor positioning based on joint TDOA and DOA estimation using 2-D matrix pencil algorithms and IEEE 802.11ac. IEEE Trans. Wirel. Commun. **14**(5), 2440–2454 (2015)
11. Hongmei, Z., Zhenguo, G., Fu, H.: High resolution random linear sonar array based MUSIC method for underwater DOA estimation. In: Proceedings of 32nd Chinese Control Conference, Xi'an, China, pp. 4592–4595, July 2013
12. Chen, L., Qi, W.: Joint 2-D DOA and TOA estimation for multipath OFDM signals based on three antennas. IEEE Commun. Lett. **22**(2), 324–327 (2018)
13. Zhang, X., Gao, X., Xu, D.: Multi-invariance ESPRIT-based blind DOA estimation for MC-CDMA with an antenna array. IEEE Trans. Veh. Technol. **58**(8), 4686–4690 (2009)

14. Kim, S., Oh, D., Lee, J.: Joint DFT-ESPRIT estimation for TOA and DOA in vehicle FMCW radars. IEEE Antennas Wirel. Propag. Lett. **14**, 1710–1713 (2015)
15. Yao, H., Tianqi, Z., Qingsha, G., et al.: A method improving the accuracy of UKF. Comput. Simul. **27**(3), 348–352 (2010)
16. Oh, D., Kim, S., Yoon, S.-H., Chong, J.-W.: Two-dimensional ESPRIT-Like shift-invariant TOA estimation algorithm using multi-band chirp signals robust to carrier frequency offset. IEEE Trans. Wirel. Commun. **12**(7), 3130–3139 (2013)